Probing the nucleoporin FG repeat network defines structural and functional features of the nuclear pore complex

Philipp Stelter, Ruth Kunze, Jessica Fischer, and Ed Hurt

Biochemie-Zentrum der Universität Heidelberg, D-69120 Heidelberg, Germany

Unraveling the organization of the FG repeat meshwork that forms the active transport channel of the nuclear pore complex (NPC) is key to understanding the mechanism of nucleocytoplasmic transport. In this paper, we develop a tool to probe the FG repeat network in living cells by modifying FG nucleoporins (Nups) with a binding motif (engineered dynein light chain–interacting domain) that can drag several copies of an interfering protein, Dyn2, into the FG network to plug the pore and stop nucleocytoplasmic transport. Our method allows us to specifically probe FG Nups in vivo, which provides insight into the organization and function of the NPC transport channel.

Introduction

The genetic information of a eukaryotic cell is enclosed by the nuclear envelope, but nuclear pore complexes (NPCs) inserted into the double nuclear membrane mediate nucleocytoplasmic transport of molecules as diverse as proteins, RNAs, and RNPs. The NPC exhibits an overall octagonal structure, 40–60 MD in size, which generates the active transport channel through which nucleocytoplasmic traffic occurs (Rout et al., 2000; Schwartz, 2005). In all eukaryotes, a group of $\sim$30 conserved nucleoporins (Nups), existing in multiple (8, 16, and 32) copies, builds up this huge assembly. A subgroup of these Nups ($\sim$30%) contains FG (Phe-Gly)-rich repeat domains, which are thought to form a network of FG repeat filaments that constitute both the permeability barrier and the active transport channel of the NPC (Peters, 2009). Because the FG repeat domains can directly interact with the shuttling transport receptors, it is assumed that these transporters loaded with cargo travel through the NPC by transient low affinity contacts with the numerous FG repeats lining the transport channel (Rexach and Blobel, 1995; Ribbeck and Görlich, 2001). Thus, knowledge of the topological organization of the FG repeat network in the NPC is crucial to gain mechanistic insight into nucleocytoplasmic transport reactions.

Biochemical and biophysical methods revealed that in vitro FG repeat domains are largely unstructured but may form a meshwork via interactions between FG repeats (Denning et al., 2003; Frey et al., 2006; Lim et al., 2007; Patel et al., 2007; Yamada et al., 2010). However, because of their natively unfolded state, the organization of such an FG repeat network within the NPC in the living cells is currently unknown. Hence, several models have been postulated, which predict how the different FG repeat domains are organized and interconnected within the NPC scaffold (Ribbeck and Görlich, 2002; Rout et al., 2003; Lim et al., 2006; Peters, 2009; Yamada et al., 2010). The selective phase model assumes a saturated FG repeat hydrogel formed by the different FG repeat domains that can be overcome by the nuclear transport receptors, which can penetrate through the hydrogel by locally dissolving the FG network (Frey et al., 2006). In another model, the Brownian affinity gating, FG domains are suggested to protrude from the NPC into the cytoplasm and nucleoplasm in a bristlelike fashion (Rout et al., 2000, 2003). Cargo-loaded receptors can bind reversibly to these FG repeats and, thus, have a high probability of entering the central transport channel. The reduction of dimensionality model (for reduction of dimensionality) suggests a coherent hydrophobic FG repeat layer coating the wall of the transport channel and the surface of the nuclear and cytoplasmic filaments. In this case, the cargo–receptor complex binds and diffuses along a two-dimensional surface formed by the FG repeat

The Rockefeller University Press $30.00
J. Cell Biol. Vol. 195 No. 2   183–192
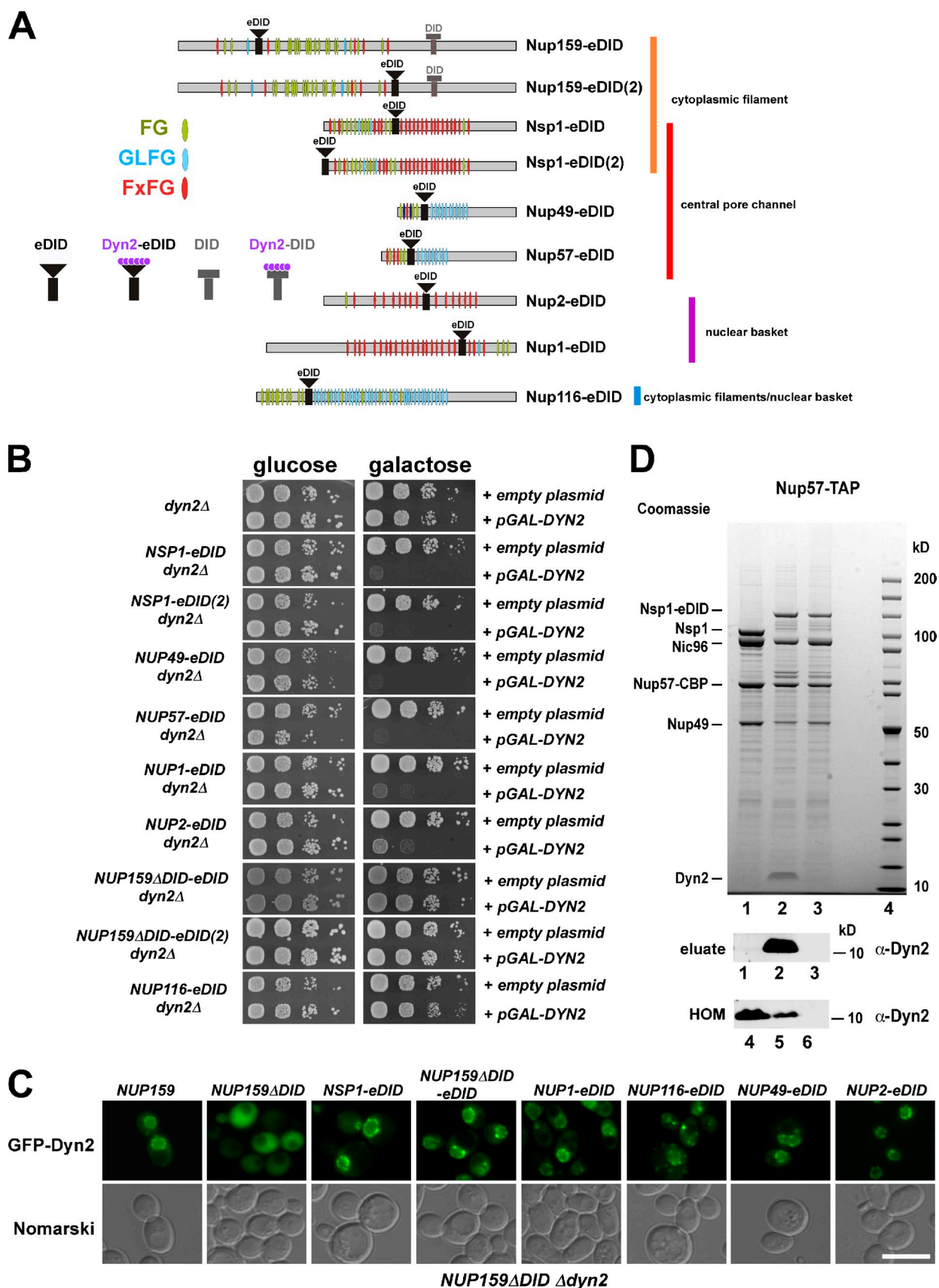www.jcb.org/cgi/doi/10.1083/jcb.201105042

JCB **183**

Figure 1. **Recruitment of Dyn2 to eDID-modified FG repeat domains of FG Nups at the NPC can cause a toxic phenotype.** (A) Schematic drawing of the FG repeat Nups tested in this study: Nup159 with its natural DID, Nup116, Nsp1, Nup49, Nup57, Nup2, and Nup1 and position of the various FG repeat motifs (FG, GLFG, and FxFG; according to Strawn et al., 2004). Also indicated is the eDID insertion site within the corresponding FG repeat domain after

domains (Peters, 2009). Recently, Yamada et al. (2010) proposed a nonrandomized arrangement of the FG repeat network, organized into two separated zones of traffic within the NPC with different physiochemical properties.

In view of these different models, it is crucial to gain insight into the topological arrangement of FG repeat domains in the NPC scaffold. Hence, we took advantage of a relatively short binding motif (Dyn2 interaction domain) that was inserted into the FG repeat domains of several FG nucleoporins. Upon induction of *GAL::DYN2*, Dyn2 molecules were recruited into the FG repeat network, thereby interfering with nucleocytoplasmic transport. Our method allows us to analyze the topological arrangement of the different FG repeat domains within the NPC scaffold.

Results and discussion

Design of a tool to probe FG repeat Nups in vivo

We sought to develop a tool for probing individual FG repeat nucleoporins in vivo to gain insight into the organization and function of the FG repeat network. Previously, we showed that under physiological conditions, Dyn2 is recruited to Nup159, a subunit of the Nup82–Nsp1–Nup159 complex located at the cytoplasmic pore filaments (Stelter et al., 2007). Specifically, Dyn2 is bound to a Dyn2 interaction motif (dynein light chain–interacting domain [DID]) present between the FG and coiled-coil domain of Nup159, generating a 20-nm elongated structure that could contribute to the formation of the cytoplasmic pore filaments (Fig. 1 A). Moreover, the Nup82 complex dimerizes via the $Nup159_{DID}$ in a Dyn2-dependent manner, which facilitates NPC assembly. Dyn2 forms only a small 20-kD dimer and, when depleted or overexpressed, in a wild-type background, does not significantly influence growth or nucleocytoplasmic transport. These characteristics, therefore, make Dyn2, which should overcome the permeability barrier of the NPC, a promising tool to probe the FG repeat network in vivo. Hence, we inserted an engineered DID (eDID) composed of six consecutive Dyn2 binding motifs (derived from Pac11; see also Flemming et al., 2010) into the FG repeat domain of different FG Nups to test for consequences in NPC function. The selected FG Nups were Nup159, Nsp1, Nup49, Nup57, Nup2, Nup1, and Nup116 (Fig. 1 A and Fig. S1 A), which are either representatives of a discrete topological location in the NPC or are part of distinct NPC modules.

Subsequently, we tested whether these eDID-FG Nups can recruit dynein light chain (Dyn2) upon *GAL-DYN2* induction.

Probing eDID-labeled FG repeat domains with Dyn2

To find out whether eDID insertion interferes with the corresponding Nup function, the eDID-modified FG domain was integrated at the corresponding chromosomal *NUP* locus (see Materials and methods) and tested for expression and complementation in the absence of chromosomal *DYN2* or upon *pGAL-DYN2* induction (Fig. 1 B). We inserted the eDID roughly in the middle of a FG repeat domain to be sufficiently away from the interaction motifs of the tested nucleoporins (e.g., coiled-coil domain of Nsp1, Nup49, and Nup159; Fig. 1 A). Moreover, the insertion in the midst of the FG repeat domain could allow for a maximal penetration of the eDID into the FG repeat network as part of the NPC transport channel. For control reasons, we also shifted the eDID toward the beginning of the FG repeats within Nsp1 (i.e., Nsp1-eDID(2)) or toward the coiled-coil domain of Nup159 (i.e., Nup159-eDID(2)). All these modified FG Nups tolerated the eDID insertion without an apparent growth inhibition (Fig. 1 B, glucose). However, we cannot exclude that the eDID insertion into the FG repeat domains can cause synergistic effects when combined with other Nup mutants.

Strikingly, induction of *GAL::DYN2* expression induced a lethal or extremely slow growth phenotype in several of the strains that harbored such an eDID-modified FG Nup. Specifically, Dyn2 expression was lethal to cells expressing Nsp1-eDID, Nup49-eDID, Nup57-eDID, Nup2-eDID, and Nup1-eDID but was not toxic in cells expressing Nup116-eDID or Nup159ΔDID-eDID (Fig. 1 B, galactose). The growth inhibition (and also the mRNA transport defects; Fig. 2 and Fig. S3 B) was not always fully complemented by coexpression of the respective wild-type Nup (Fig. S3). These data suggest some dominant effect of these Nup-eDID constructs with respect to growth and/or nucleocytoplasmic transport.

To demonstrate that eDID-labeled FG repeat domains can recruit Dyn2 to the NPC, we analyzed cells expressing GFP-labeled Dyn2 by fluorescence microscopy. For this purpose, we deleted the endogenous DID from Nup159 so that we could monitor NPC targeting of Dyn2-GFP mediated by another eDID-modified FG Nup. As anticipated, Dyn2-GFP was not detected at the nuclear envelope in a *NUP159ΔDID* strain (see also Stelter et al., 2007) but exhibited a punctate nuclear envelope labeling characteristic of an NPC localization when the

Cre-induced recombination (Nup159ΔDID-eDID[624; i.e., insertion at amino acid position 624], Nup159ΔDID-eDID(2)[904], Nsp1-eDID[275], Nsp1-eDID(2)[2], Nup49-eDID[81], Nup57-eDID[71], Nup2-eDID[407], Nup1-eDID[717], and Nup116-eDID[197]) and recruitment of six Dyn2 molecules (violet) to the eDID platform. The topological position of the various FG Nups within the NPC scaffold is also drawn. (B) Growth of *dyn2Δ* strains that carry the wild-type *NUP* in a *dyn2*-null background (*dyn2Δ*) or the indicated eDID-labeled FG repeat Nup, transformed with either an empty *pGAL* plasmid (empty plasmid) or a plasmid containing *pGAL-DYN2*. *pGAL-DYN2* was repressed in glucose medium and induced in galactose medium. Growth was analyzed on SDC-Leu (glucose) or SGC-Leu (galactose) plates after 2 and 3 d, respectively. (C) Subcellular localization of *pGAL-DYN2*-GFP after 30-min galactose induction in *NUP159ΔDID dyn2Δ NUP-eDID* strains. *NUP159 dyn2Δ + pGAL-DYN2*-GFP and *NUP159ΔDID dyn2Δ + pGAL-DYN2*-GFP strains served as positive and negative controls, respectively. Fluorescence microscopy and Nomarski micrographs of representative cells are shown. Bar, 5 µm. (D) TAP of Nup57-TAP from strain *dyn2Δ NSP1-eDID* (lane 3) or *dyn2Δ NSP1-eDID + GAL::DYN2* (lane 2) after 3-h galactose induction. Nup57-TAP affinity purified from wild-type + *GAL::DYN2* (lane 1) cells served as a control after 3 h galactose induction. Calmodulin beads and whole-cell lysates (homogenates [HOM], lanes 4–6) were boiled in sample buffer and analyzed by SDS-PAGE and Coomassie staining or Western blotting using anti-Dyn2 antibodies. CBP, calmodulin-binding peptide.
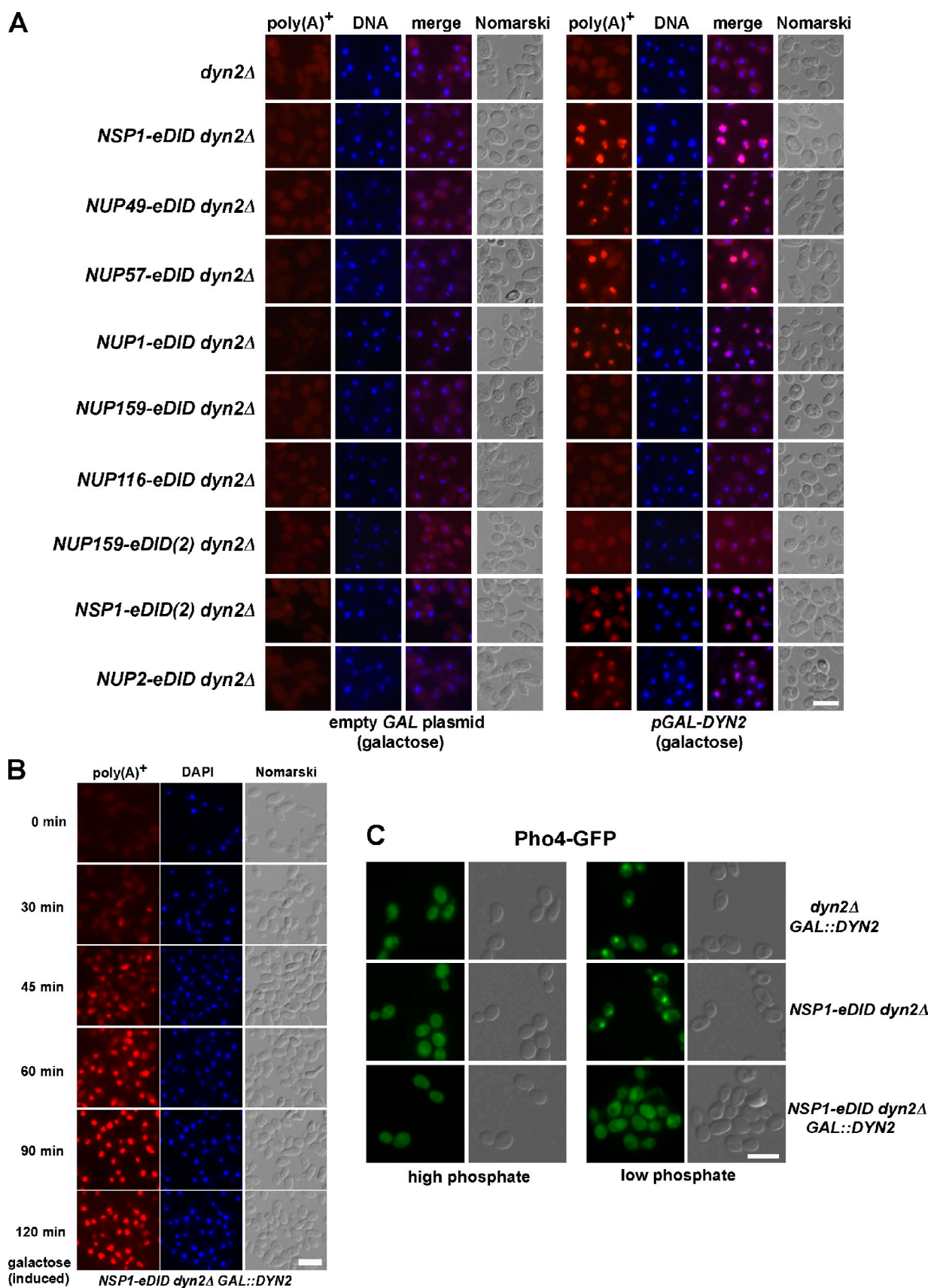
Figure 2.   **Recruitment of Dyn2 to eDID-modified FG repeat Nups can cause inhibition of nuclear import and export processes.** (A) Analysis of nuclear mRNA export after 2-h galactose induction of Dyn2 expression in the indicated *eDID-FG* repeat *NUP* strains harboring an empty *GAL* plasmid (left) or *pGAL-DYN2* (right). Poly(A)⁺ RNA was analyzed by in situ hybridization with a Cy3-labeled oligo d(T) probe, and DNA was stained with DAPI. (B) Time

eDID was inserted into the FG repeat domains of Nsp1, Nup159, Nup49, Nup1, and Nup2 (Fig. 1 C). Nup116-eDID also recruited Dyn2 to the NPC but less efficiently than the other constructs (Fig. 1 C).

To follow Dyn2 recruitment to the eDID-modified Nups biochemically, we performed affinity purification. First, we focused on Nsp1, which is part of two NPC modules: (1) the Nsp1–Nup82–Nup159 complex located at the cytoplasmic pore filaments and (2) the Nsp1–Nup49–Nup57–Nic96 complex present in the central pore channel (Grandi et al., 1993, 1995; Hurwitz and Blobel, 1995; Fahrenkrog et al., 1998). To demonstrate that Dyn2 can reach not only the peripheral but also the central NPC module, we affinity purified tandem affinity purification (TAP)–tagged Nup57 from the *NSP1-eDID* strain under conditions of *GAL::DYN2* repression or expression. Affinity-purified Nup57 containing Nsp1-eDID, Nic96, and Nup49 was coenriched in Dyn2, suggesting that dynein light chain can penetrate into the central pore channel that contains the Nsp1–Nup57–Nup49 complex (Fig. 1 D). In addition to these biochemical data obtained from the Nsp1-eDID cells, we affinity purified the other eDID-modified Nups (either directly via the TAP tag or via an interacting TAP-tagged Nup). This analysis revealed a significant Dyn2 recruitment after 3 h of Dyn2 induction, independent of whether the eDID-Nup was sensitive to Dyn2 expression or not (Fig. S1 C). To determine whether Dyn2 can dimerize the eDID-modified Nups, we performed coexpression experiments of GFP-Nup82 and GFP-Nic96, in the presence or absence of Dyn2, in *NUP82*-TAP *NUP159-eDID* and *NIC96*-TAP *NUP49-eDID* strains, respectively. Affinity purification of the TAP-tagged proteins revealed a certain degree of Dyn2-dependent dimerization of these complexes (Fig. S1 D). Collectively, these data suggest that all of the tested eDID-labeled bait proteins significantly coenriched Dyn2, independent of whether the eDID-FG repeat construct caused inhibition of mRNA export or not. Thus, Dyn2 gains access to the eDID-modified Nups assembled into the NPC scaffold.

Recruitment of Dyn2 to eDID-FG repeat domains blocks nucleocytoplasmic transport

Next, we wanted to find out why cell growth stops when Dyn2 is recruited to a distinct group of eDID-modified FG Nups. We hypothesized that this could be a result of a blockage of nucleocytoplasmic transport caused by corrupting the FG repeat network in the active transport channel with Dyn2 molecules. Strikingly, nuclear mRNA export was massively inhibited after an induction of *pGAL-DYN2* expression in the nonviable *NSP1*-eDID, *NSP1*-eDID(2), *NUP49*-eDID, *NUP57*-eDID, *NUP1*-eDID, and *NUP2*-eDID cells but not in the viable *NUP116*-eDID, *NUP159 ΔDID*-eDID, and *NUP159ΔDID*-eDID(2) cells (Fig. 2 A).

The onset of this defect is very fast and could already be well observed after a 45-min shift to galactose medium (note that it requires ∼20–30 min to initiate *GAL* promoter-induced protein expression) and, hence, is indicative of a direct transport inhibition rather than an NPC assembly defect (Fig. 2 B). Both, poly(A)$^+$ RNA as well as specific mRNAs (e.g., actin and SSA1 heat shock mRNAs) that accumulate in the nucleus tend to cluster in foci that are close to the nuclear envelope (Fig. 2, A and B; and Fig. 3).

We performed EM to reveal the perinuclear poly(A)$^+$ accumulation at the ultrastructural level. In this case, a network of electron-dense particles, which could correspond to accumulated mRNA RNPs and/or a mixture of several RNA/RNP/protein aggregates, were often lining the inner nuclear membrane, with several particles in close proximity to NPCs (Fig. 3). We interpret these data to suggest that upon recruitment of Dyn2 molecules to eDID-modified FG repeat Nups, the NPC transport channel becomes blocked, thus explaining the observed perinuclear accumulation of RNP/protein aggregates.

Consistent with a plugged pore channel, we observe inhibition of other nucleocytoplasmic transport processes in the toxic Nsp1-eDID, Nup49-eDID, Nup57-eDID, and Nup1-eDID strains after *GAL::DYN2* induction. A defect in ribosomal 60S and 40S subunit export in these arrested cells was indicated by nuclear accumulation of the large subunit reporter Rpl25-GFP (Fig. S2 A) and appearance of the 20S preribosomal RNA (pre-rRNA) intermediate in the nucleoplasm, respectively (Fig. S2 B). Interestingly, NUP2-eDID exhibited a pronounced mRNA transport defect but less of a mislocation of the ITS1 pre-rRNA (Fig. 2 A and Fig. S2 B). Moreover, nuclear protein import was impaired, as revealed by the inability of the Pho4-GFP reporter to enter the nucleus in the *NSP1*-eDID strain expressing Dyn2 (Fig. 2 C). Collectively, recruitment of Dyn2 to the FG repeat domains of several Nups induces inhibition of the major nucleocytoplasmic transport pathways.

Relocation of eDID-modified FG repeat domains to distinct NPC topological positions changes sensitivity toward Dyn2 expression

The data so far did not allow discrimination between whether the FG repeat domain modified with Dyn2 blocks nucleocytoplasmic transport because of the type of FG repeats or the topological location within the NPC scaffold. To distinguish between these possibilities, we sought to change the localization of eDID-FG repeat domains by genetic engineering. Hence, we replaced the FG repeat domain of Nup159 (putative "nontoxic" location) or Nup57 (putative "toxic" location) with the eDID-FG domain of Nsp1 (Fig. 4 A). Both chimera, Nup57-eDID-FG$_{Nsp1}$ and Nup159ΔDID-eDID-FG$_{Nsp1}$, were

---

course of nuclear poly(A)$^+$ accumulation in logarithmically growing *NSP1-eDID dyn2Δ* cells expressing Dyn2 from integrated *GAL::DYN2*. Cells were grown in YPR to an OD of ∼0.5 before Dyn2 expression was induced by adding 2% galactose. After the indicated time points, samples were taken and fixed by adding 4% formaldehyde to the culture medium. Samples were further processed for in situ poly(A)$^+$ hybridization (see Materials and methods). (C) Analysis of nuclear import of Pho4-GFP in the *dyn2Δ* and *NSP1-eDID dyn2Δ* strains lacking or harboring the chromosomal integrated *GAL::DYN2*. Cells were grown in high phosphate medium followed by 2-h galactose induction of the *GAL::DYN2* and switched to low phosphate medium. Pho4-GFP import was analyzed after 1 h in the fluorescence microscope. Bars, 5 µm.
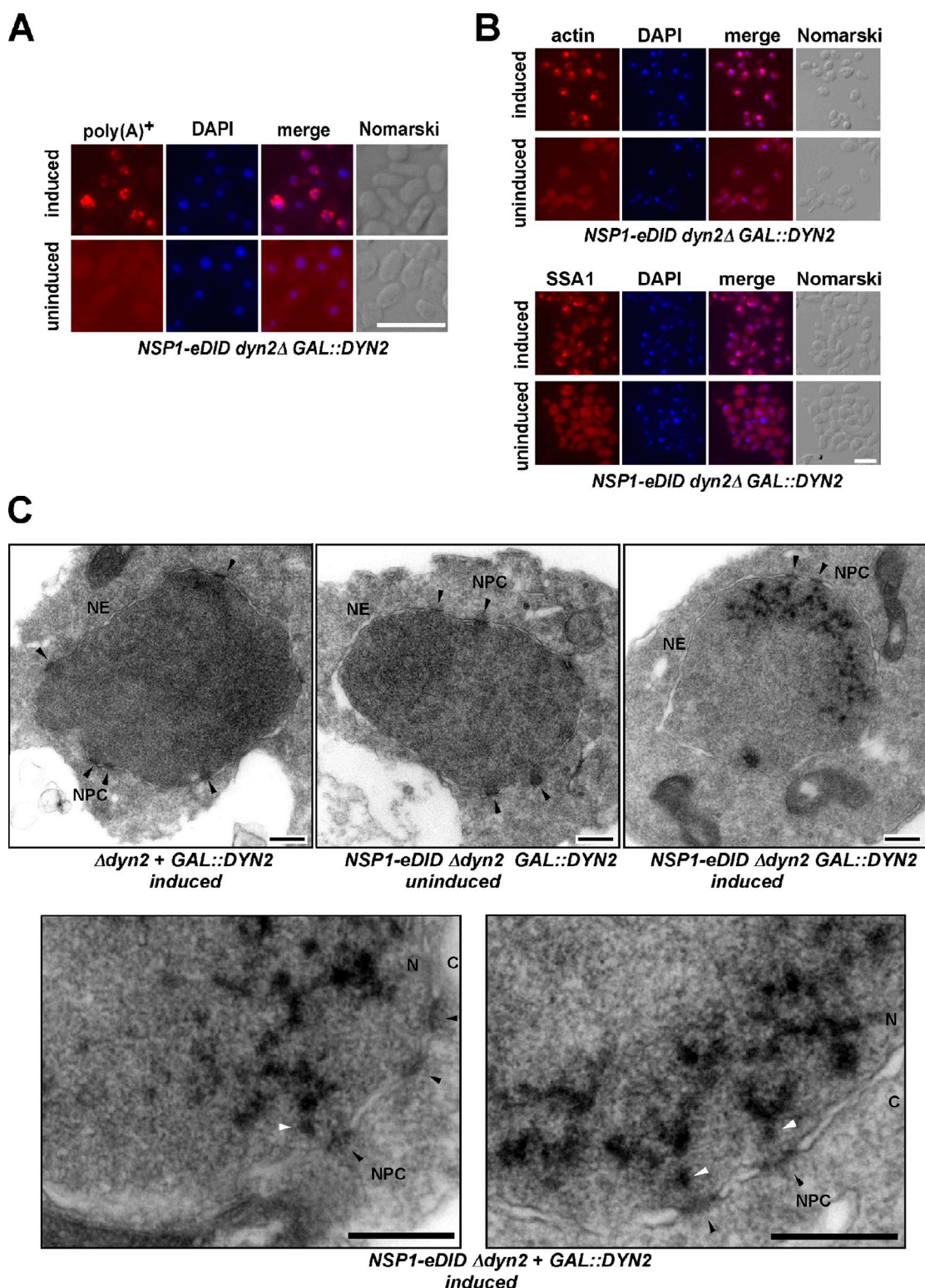
Figure 3. **Perinuclear accumulation of material in cells expressing Nsp1-eDID with bound Dyn2.** (A) Perinuclear accumulation of poly(A)⁺ RNA in the *NSP1-eDID* cells harboring the chromosomal integrated *GAL::DYN2* after shift from raffinose to galactose medium that was induced (2 h in galactose) and uninduced (0 h in galactose). The indicated RNA was detected by in situ hybridization using appropriate Cy3-labeled RNA probes. DNA was stained with DAPI. (B) Analysis of nuclear export of specific mRNAs encoding actin and SSA1 proteins in the *NSP1-eDID dyn2Δ* strain harboring the integrated *GAL::DYN2* after shift from raffinose to galactose medium. 0 h in galactose (uninduced); 2 h in galactose (induced). The indicated RNA was detected by in situ hybridization using appropriate Cy3-labeled RNA probes. DNA was stained with DAPI. For the detection of SSA1 mRNA, cells were shifted to 37°C for 30 min before cells were fixed and further processed. (C) Transmission EM of thin-sectioned yeast cells expressing the eDID-modified FG repeat domain of Nsp1 with bound Dyn2. (top) Overview micrographs of representative cells are shown derived from strains *dyn2Δ + GAL::DYN2* and *NSP1-eDID dyn2Δ + GAL::DYN2* in an uninduced and Dyn2-induced condition. (bottom) Higher magnification EM micrographs showing strain *NSP1-eDID dyn2Δ + GAL::DYN2* in the Dyn2-induced condition. NPC, nuclear pore complex (filled arrowhead); NE, nuclear envelope; N, nucleus; C, cytoplasm. White arrowheads indicate electron-dense particles accumulating in the perinuclear region with some particles close to an NPC. Bars: (A and B) 5 µm; (C) 250 nm.
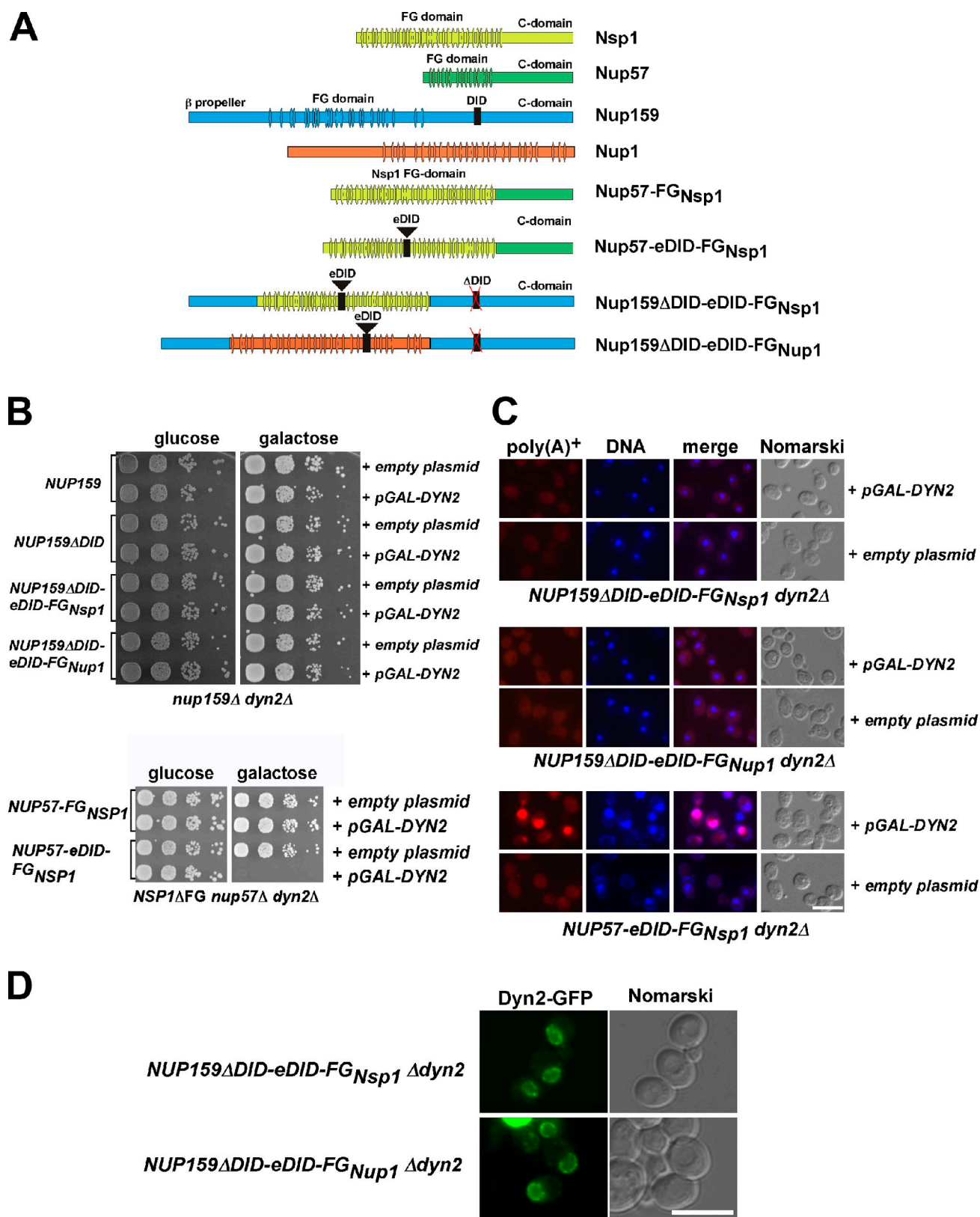
Figure 4. **Transplantation of the eDID-FG repeat domain from Nsp1 and Nup1 onto Nup159 causes a loss of toxicity toward Dyn2 expression.** (A) Schematic drawing of the involved FG repeat Nups, the transplantation of the indicated eDID-labeled FG_Nsp1 repeat domain onto Nup57, and the eDID-labeled FG_Nsp1 or FG_Nup1 repeat domain onto Nup159. C-domain, C-terminal domain. (B) To analyze the effect of Dyn2 expression, strains were transformed with an empty plasmid or *pGAL-DYN2*. The indicated cells were plated on SDC (glucose) and SGC (galactose) plates, and growth was analyzed after 2 and 3 d, respectively. (C) Poly(A)+ RNA export was analyzed after 3-h Dyn2 induction by in situ hybridization using a Cy3-labeled oligo d(T) probe. (D) Subcellular localization of *pGAL-DYN2*-GFP was analyzed in the *NUP159ΔDID-eDID-FG_Nsp1 Δdyn2* and *NUP159ΔDID-eDID-FG_Nup1 Δdyn2* strain after 30-min galactose induction. Bars, 5 µm.

functional and complemented the respective null mutants *nup57Δ* and *nup159Δ* (Fig. 4 B). Interestingly, the eDID-FG$_{Nsp1}$ attached to Nup57 still yielded a robust growth and mRNA export defect upon Dyn2 expression. However, when the eDID-FG$_{Nsp1}$ or the eDID-FG$_{Nup1}$ was transplanted onto Nup159, neither defective mRNA export nor growth inhibition was observed (Fig. 4, B and C; and Fig. S1 E). Affinity purification of Nup82-TAP from strain *NUP159ΔDID-eDID-FG$_{Nsp1}$* showed that Dyn2 was recruited to this NPC module of the cytoplasmic pore filaments upon *GAL::DYN2* expression (not depicted), which could also be confirmed by GFP-Dyn2 location experiments (Fig. 4 D). These data indicate separate roles of the unique Nsp1 FG repeat domain, which is part of two distinct NPC subcomplexes. Accordingly, the peripheral FG repeat domains of Nup159 and Nsp1 as part of the Nup82 complex may protrude into the cytoplasm to be used for recruitment of nuclear import receptors or termination of nuclear mRNA export (Stelter et al., 2007). Whereas the chemically identical other Nsp1 FG repeat protruding from the Nsp1–Nup49–Nup57 complex is crucially involved in lining the central transport channel to generate the permeability barrier.

In summary, we describe a method that allows probing the different FG repeat–containing Nups in vivo to gain insight into their topological arrangement in the NPC. In the past, the in vivo role of FG repeats for NPC structure and function was studied by deleting large parts of the FG repeat domains in yeast (Nehrbass et al., 1990; Strawn et al., 2004) or by generating mutations (Frey et al., 2006). Our newly developed tool to manipulate FG repeats in vivo depends on the recruitment of (theoretically six) Dyn2 homodimers to a specific FG repeat domain that carries a row of Dyn2 binding motifs. Upon binding of Dyn2 to the eDID-FG Nup, the in vivo function of this FG repeat domain could be manipulated in a way that massively blocked nucleocytoplasmic transport. It appears that eDID-carrying FG repeats that belong to Nups of the central transport channel (e.g., Nsp1 and Nup57) or the nuclear basket (e.g., Nup1 and Nup2) cause a massive nucleocytoplasmic transport defect upon Dyn2 binding. However, probing eDID-FG repeats that are physically linked to the cytoplasmic pore filaments (i.e., Nup159) with Dyn2 did not interfere with nucleocytoplasmic transport. For Nup116-eDID, we cannot make a firm conclusion because the eDID insertion partly impaired assembly into the NPC.

We assume that binding of Dyn2 homodimers to eDID-modified FG repeat domains generates a bulky structure (the DID-Dyn2 assembly forms a ∼20-nm-long rod in vitro; see Stelter et al., 2007) that plugs the NPC transport channel and restricts passage of the cargo-loaded receptor (e.g., karyopherins, an mRNA exporter) through the FG repeat network. In addition, Dyn2 homodimers can cross-link neighboring eDID-modified FG repeats (also see Stelter et al., 2007), further impairing passage of transport receptors through the FG meshwork. We suggest exploiting this approach further as biochemical (e.g., purification), cell biology (e.g., Förster resonance energy transfer), and genetic tool (e.g., mutant screen) for probing not only the NPC but also other macromolecular machines.

Materials and methods

Construction of yeast strains and growth

Chromosomal integration of the eDID-Flag-LoxP motif (LoxP for subsequent deletion of the selectable marker from the eDID-Flag site by Cre recombinase–induced recombination; Fig. S1, amino acid sequence) into the various FG repeat domains of FG Nups was performed in the *dyn2Δ* (*MATα leu2-Δ1 trp1-Δ63 his3-Δ300 ura3-52 dyn2::LoxP*) or *NUP159ΔDID dyn2Δ* strain (*MATα trp1-1 his3-11,15 ura3-52 leu2-3 ade2-112 nup159::KanMX dyn2::KanMX pRS414-NUP159ΔDID*). The eDID-Flag-LoxP construct was cloned into a pFa6a vector yielding pFa6a-LoxP-eDID-Flag-LoxP::*HisMX4*, which was used as the template for the respective integration PCRs. Integration of the eDID-Flag-LoxP was performed in the different yeast strains in the presence of a plasmid-based wild-type copy of the corresponding *NUP* gene to be targeted with eDID-Flag. Deletion of the *HisMX4* cassette and the resulting in-frame fusion of the eDID-Flag with the respective FG domains were performed using Cre recombinase (Baudin et al., 1993). Correct integration of the eDID-Flag label at the corresponding *NUP* locus and expression of the eDID-modified Nup was verified by Western blot analysis of whole-cell lysates using anti-Flag antibodies. In these strains, Dyn2 was expressed from a *pGAL-DYN2* plasmid or from a chromosomally integrated *GAL::DYN2*. To analyze the GFP-Dyn2 localization in the eDID-*NUP* strains, we transformed these strains with a *NUP159* shuffle plasmid and deleted the chromosomal *NUP159* gene with a *HisMX4* cassette. These strains were transformed with pRS414-*NUP159ΔDID* and shuffled on 5-fluoroorotic acid. Growth was analyzed on YPD (yeast peptone dextrose; glucose), YPR (yeast peptone raffinose), or YPG (yeast peptone galactose) plates as well as on minimal synthetic dextrose complete (SDC) versus synthetic galactose complete (SGC) plates. Additional strains and plasmids used in this study are listed in Table S1 and Table S2.

Analysis of nucleocytoplasmic transport in yeast cells

Analysis of nuclear mRNA export was performed by fluorescence in situ hybridization as previously described (Doye et al., 1994). In brief, cells were grown in SDC-Leu medium and transferred to YPR medium for 4 h before 2% galactose was added for the indicated time points. Nuclear accumulation of poly(A)$^+$ RNA or distribution of ITS1-containing pre-RNAs was determined using Cy3-labeled oligo(dT) or 5′-Cy3-ATGCTCTTGC-CAAAACAAAAAAATCCATTTTCAAAATTATTAAATTTCTT-3′ probes, respectively. Nuclear accumulation of actin mRNA was analyzed with Cy3-labeled actin probe (Sträßer and Hurt, 2001). SSA1 mRNA export was analyzed in logarithmically growing cells incubated with 2% galactose medium for 1.5 h to induce Dyn2 followed by a further shift to 37°C for 30 min to induce SSA1 expression. SSA1 mRNA was detected using the Cy3-labeled DNA probe (Sträßer and Hurt, 2001). Nuclear export of the ribosomal 40S subunit was followed by fluorescence in situ hybridization, as previously described, using a Cy3-labeled ITS1-specific probe for detection of ITS1-containing pre-rRNAs (Pertschy et al., 2009). Export of the ribosomal 60S subunit was monitored using the Rpl25-EGFP reporter (Gadal et al., 2001). Cells were grown in SDC-Leu/-Ura medium overnight and transferred to YPR medium for 4 h. Dyn2 was induced for the indicated time points, and the Rpl25-EGFP, Nop1-monomeric RFP (mRFP), and DAPI distributions were examined by fluorescence microscopy using a microscope (Imager Z1; Carl Zeiss) with a 63 or 100×, NA 1.4 Plan Apochromat oil immersion lens (Carl Zeiss) and differential interference contrast, humanized EGFP, DAPI, mRFP, or HECy3 filter sets. Pictures were acquired with a camera (AxioCam MRm; Carl Zeiss) and Axio-Vision 4.3 software (Carl Zeiss). Analysis of the subcellular Dyn2 location was performed in the *NUP159ΔDID dyn2Δ NUP-eDID* strains transformed with the plasmid *pGAL-DYN2*-GFP. Cells were induced for 30 min in galactose medium, and expression was subsequently stopped by adding glucose. The GFP-Dyn2 localization was analyzed after 1 h by fluorescence microscopy.

Nuclear import of the chromosomal GFP-tagged Pho4 was examined, as previously described (Kaffman et al., 1998), in the yeast strains *NSP1-eDID dyn2Δ*, *NSP1-eDID dyn2Δ GAL::DYN2*, and *dyn2Δ GAL::DYN2*. Cells were grown at 30°C overnight in SRC + all medium supplemented with 11 mM KH$_2$PO$_4$ (high phosphate) to an OD of ∼0.1–0.2 before galactose was added to a final concentration of 2% for an additional 3 h. Finally, cells were centrifuged and washed twice in water and in low phosphate medium (SRC + all medium + 220 µM KH$_2$PO$_4$) before being resuspended in low phosphate medium followed by a further incubation for 1 h at 30°C. Pho4-GFP import was analyzed in the fluorescence microscope.

Affinity purification of TAP-tagged Nups

Affinity purification of TAP-tagged bait proteins was performed as previously described (Puig et al., 2001). In brief, cells were broken in standard purification buffer containing 150 mM NaCl, 50 mM K(OAc), 20 mM Tris-HCl, 2 mM Mg(OAc), and 0.1% NP-40, pH 7.5, in a mill (PULVERISETTE; FRITSCH), extracts were centrifuged for 10 min at 3,400 g, and the supernatant was further centrifuged at 35,000 g for 20 min. The supernatant was incubated with 300 µl IgG (GE Healthcare) slurry at 4°C for 1 h. IgG beads with bound proteins were washed several times with purification buffer. Tobacco etch virus cleavage was performed at 16°C for 90 min in purification buffer. Tobacco etch virus eluates were supplemented with CaCl$_2$ to a final concentration of 1 mM and incubated with calmodulin beads (GE Healthcare) for 60 min at 4°C. Calmodulin beads with the bound protein complexes were treated with SDS sample buffer and analyzed by SDS-PAGE, Coomassie staining, or Western blotting. Antibodies raised against recombinant Dyn2 were made in rabbit (Stelter et al., 2007). TAP-tagged strains were grown overnight to an OD of 1.5, and galactose was added to a final volume of 2% for an additional 3 h before affinity purification.

Thin-section EM

The yeast cells were fixed with 2% formaldehyde/2% glutaraldehyde for 45 min on ice. After spheroblasting, postfixation with osmium tetroxide, and contrasting en bloc with uranyl acetate, they were dehydrated with a graded series of ethanol and embedded in glycid ether 100–based resin. After polymerization at 60°C, ultrathin sections were cut with an ultramicrotome (Ultracut S; Reichert). They were contrasted with uranyl acetate and lead citrate and examined in a transmission electron microscope (EM 10 CR; Carl Zeiss) at an acceleration voltage of 60 kV.

Miscellaneous

Integration of the TAP cassette at the *NUP57*, *NUP49*, *NUP116*, *NUP60*, *NUP1*, *Nic96*, or *NUP82* chromosomal locus in the indicated yeast strains was performed as previously described (Puig et al., 1998; Janke et al., 2004).

Online supplemental material

Fig. S1 shows Dyn2 recruitment to eDID-labeled FG domain Nups. Ribosomal export was analyzed in Fig. S2. Fig. S3 shows analysis of growth and nucleocytoplasmic transport of *NUP-eDID* + pGAL-DYN2 strains transformed with the respective wild-type Nups. Table S1 and Table S2 include yeast strains and plasmids used in this study, respectively. Online supplemental material is available at http://www.jcb.org/cgi/content/full/jcb.201105042/DC1.

References

Baudin, A., O. Ozier-Kalogeropoulos, A. Denouel, F. Lacroute, and C. Cullin. 1993. A simple and efficient method for direct gene deletion in *Saccharomyces cerevisiae*. *Nucleic Acids Res.* 21:3329–3330. http://dx.doi.org/10.1093/nar/21.14.3329

Denning, D.P., S.S. Patel, V. Uversky, A.L. Fink, and M. Rexach. 2003. Disorder in the nuclear pore complex: the FG repeat regions of nucleoporins are natively unfolded. *Proc. Natl. Acad. Sci. USA*. 100:2450–2455. http://dx.doi.org/10.1073/pnas.0437902100

Doye, V., R. Wepf, and E.C. Hurt. 1994. A novel nuclear pore protein Nup133p with distinct roles in poly(A)+ RNA transport and nuclear pore distribution. *EMBO J.* 13:6062–6075.

Fahrenkrog, B., E.C. Hurt, U. Aebi, and N. Panté. 1998. Molecular architecture of the yeast nuclear pore complex: Localization of Nsp1p subcomplexes. *J. Cell Biol.* 143:577–588. http://dx.doi.org/10.1083/jcb.143.3.577

Flemming, D., K. Thierbach, P. Stelter, B. Böttcher, and E. Hurt. 2010. Precise mapping of subunits in multiprotein complexes by a versatile electron microscopy label. *Nat. Struct. Mol. Biol.* 17:775–778. http://dx.doi.org/10.1038/nsmb.1811

Frey, S., R.P. Richter, and D. Görlich. 2006. FG-rich repeats of nuclear pore proteins form a three-dimensional meshwork with hydrogel-like properties. *Science*. 314:815–817. http://dx.doi.org/10.1126/science.1132516

Gadal, O., D. Strauss, J. Kessl, B. Trumpower, D. Tollervey, and E. Hurt. 2001. Nuclear export of 60S ribosomal subunits depends on Xpo1p and requires a NES-containing factor Nmd3p that associates with the large subunit protein Rpl10p. *Mol. Cell. Biol.* 21:3405–3415. http://dx.doi.org/10.1128/MCB.21.10.3405-3415.2001

Grandi, P., V. Doye, and E.C. Hurt. 1993. Purification of NSP1 reveals complex formation with 'GLFG' nucleoporins and a novel nuclear pore protein NIC96. *EMBO J.* 12:3061–3071.

Grandi, P., S. Emig, C. Weise, F. Hucho, T. Pohl, and E.C. Hurt. 1995. A novel nuclear pore protein Nup82p which specifically binds to a fraction of Nsp1p. *J. Cell Biol.* 130:1263–1273. http://dx.doi.org/10.1083/jcb.130.6.1263

Hurwitz, M.E., and G. Blobel. 1995. NUP82 is an essential yeast nucleoporin required for poly(A)+ RNA export. *J. Cell Biol.* 130:1275–1281. http://dx.doi.org/10.1083/jcb.130.6.1275

Janke, C., M.M. Magiera, N. Rathfelder, C. Taxis, S. Reber, H. Maekawa, A. Moreno-Borchart, G. Doenges, E. Schwob, E. Schiebel, and M. Knop. 2004. A versatile toolbox for PCR-based tagging of yeast genes: new fluorescent proteins, more markers and promoter substitution cassettes. *Yeast*. 21:947–962. http://dx.doi.org/10.1002/yea.1142

Kaffman, A., N.M. Rank, and E.K. O'Shea. 1998. Phosphorylation regulates association of the transcription factor Pho4 with its import receptor Pse1/Kap121. *Genes Dev.* 12:2673–2683. http://dx.doi.org/10.1101/gad.12.17.2673

Lim, R.Y., N.P. Huang, J. Köser, J. Deng, K.H. Lau, K. Schwarz-Herion, B. Fahrenkrog, and U. Aebi. 2006. Flexible phenylalanine-glycine nucleoporins as entropic barriers to nucleocytoplasmic transport. *Proc. Natl. Acad. Sci. USA*. 103:9512–9517. http://dx.doi.org/10.1073/pnas.0603521103

Lim, R.Y., B. Fahrenkrog, J. Köser, K. Schwarz-Herion, J. Deng, and U. Aebi. 2007. Nanomechanical basis of selective gating by the nuclear pore complex. *Science*. 318:640–643. http://dx.doi.org/10.1126/science.1145980

Nehrbass, U., H. Kern, A. Mutvei, H. Horstmann, B. Marshallsay, and E.C. Hurt. 1990. NSP1: a yeast nuclear envelope protein localized at the nuclear pores exerts its essential function by its carboxy-terminal domain. *Cell*. 61:979–989. http://dx.doi.org/10.1016/0092-8674(90)90063-K

Patel, S.S., B.J. Belmont, J.M. Sante, and M.F. Rexach. 2007. Natively unfolded nucleoporins gate protein diffusion across the nuclear pore complex. *Cell*. 129:83–96. http://dx.doi.org/10.1016/j.cell.2007.01.044

Pertschy, B., C. Schneider, M. Gnädig, T. Schäfer, D. Tollervey, and E. Hurt. 2009. RNA helicase Prp43 and its co-factor Pfa1 promote 20 to 18 S rRNA processing catalyzed by the endonuclease Nob1. *J. Biol. Chem.* 284:35079–35091. http://dx.doi.org/10.1074/jbc.M109.040774

Peters, R. 2009. Translocation through the nuclear pore: Kaps pave the way. *Bioessays*. 31:466–477. http://dx.doi.org/10.1002/bies.200800159

Puig, O., B. Rutz, B.G. Luukkonen, S. Kandels-Lewis, E. Bragado-Nilsson, and B. Séraphin. 1998. New constructs and strategies for efficient PCR-based gene manipulations in yeast. *Yeast*. 14:1139–1146. http://dx.doi.org/10.1002/(SICI)1097-0061(19980915)14:12<1139::AID-YEA306>3.0.CO;2-B

Puig, O., F. Caspary, G. Rigaut, B. Rutz, E. Bouveret, E. Bragado-Nilsson, M. Wilm, and B. Séraphin. 2001. The tandem affinity purification (TAP) method: a general procedure of protein complex purification. *Methods*. 24:218–229. http://dx.doi.org/10.1006/meth.2001.1183

Rexach, M., and G. Blobel. 1995. Protein import into nuclei: association and dissociation reactions involving transport substrate, transport factors, and nucleoporins. *Cell*. 83:683–692. http://dx.doi.org/10.1016/0092-8674(95)90181-7

Ribbeck, K., and D. Görlich. 2001. Kinetic analysis of translocation through nuclear pore complexes. *EMBO J.* 20:1320–1330. http://dx.doi.org/10.1093/emboj/20.6.1320

Ribbeck, K., and D. Görlich. 2002. The permeability barrier of nuclear pore complexes appears to operate via hydrophobic exclusion. *EMBO J.* 21:2664–2671. http://dx.doi.org/10.1093/emboj/21.11.2664

Rout, M.P., J.D. Aitchison, A. Suprapto, K. Hjertaas, Y. Zhao, and B.T. Chait. 2000. The yeast nuclear pore complex: composition, architecture, and transport mechanism. *J. Cell Biol.* 148:635–651. http://dx.doi.org/10.1083/jcb.148.4.635

Rout, M.P., J.D. Aitchison, M.O. Magnasco, and B.T. Chait. 2003. Virtual gating and nuclear transport: the hole picture. *Trends Cell Biol.* 13:622–628. http://dx.doi.org/10.1016/j.tcb.2003.10.007

Schwartz, T.U. 2005. Modularity within the architecture of the nuclear pore complex. *Curr. Opin. Struct. Biol.* 15:221–226. http://dx.doi.org/10.1016/j.sbi.2005.03.003

Stelter, P., R. Kunze, D. Flemming, D. Höpfner, M. Diepholz, P. Philippsen, B. Böttcher, and E. Hurt. 2007. Molecular basis for the functional

interaction of dynein light chain with the nuclear-pore complex. *Nat. Cell Biol.* 9:788–796. http://dx.doi.org/10.1038/ncb1604

Sträßer, K., and E. Hurt. 2001. Splicing factor Sub2p is required for nuclear mRNA export through its interaction with Yra1p. *Nature*. 413:648–652. http://dx.doi.org/10.1038/35098113

Strawn, L.A., T. Shen, N. Shulga, D.S. Goldfarb, and S.R. Wente. 2004. Minimal nuclear pore complexes define FG repeat domains essential for transport. *Nat. Cell Biol.* 6:197–206. http://dx.doi.org/10.1038/ncb1097

Yamada, J., J.L. Phillips, S. Patel, G. Goldfien, A. Calestagne-Morelli, H. Huang, R. Reza, J. Acheson, V.V. Krishnan, S. Newsam, et al. 2010. A bimodal distribution of two distinct categories of intrinsically disordered structures with separate functions in FG nucleoporins. *Mol. Cell. Proteomics*. 9:2205–2224. http://dx.doi.org/10.1074/mcp.M000035-MCP201